Universality classes in isotropic, Abelian, and non-Abelian sandpile models

Erel Milshtein,* Ofer Biham,† and Sorin Solomon‡
Racah Institute of Physics, The Hebrew University, Jerusalem 91904, Israel
(Received 9 February 1998)

Universality in isotropic, Abelian, and non-Abelian, sandpile models is examined using extensive numerical simulations. To characterize the critical behavior we employ an extended set of critical exponents, geometric features of the avalanches, as well as scaling functions describing the time evolution of average quantities such as the area and size during the avalanche. Comparing between the Abelian Bak-Tang-Wiesenfeld model [P. Bak, C. Tang, and K. Wiensenfeld, Phys. Rev. Lett. **59**, 381 (1987)] and the non-Abelian models introduced by Manna [S. S. Manna, J. Phys. A **24**, L363 (1991)] and Zhang [Y. C. Zhang, Phys. Rev. Lett. **63**, 470 (1989)] we find strong indications that each one of these models belongs to a distinct universality class. [S1063-651X(98)09007-2]

PACS number(s): 05.70.Jk, 05.40.+j, 05.70.Ln

I. INTRODUCTION

Sandpile models have been studied extensively during the past decade as a paradigm of self-organized criticality (SOC). This concept, introduced by Bak, Tang, and Wiesenfeld (BTW) [1,2], stimulated numerous theoretical [3–14], numerical [15–22] and experimental studies [23–28]. In sandpile models, which are defined on a lattice, grains are deposited randomly until the height at some site exceeds a threshold, and becomes unstable. Grains are then distributed to the nearest neighbors. As a result of this relaxation process, neighboring sites may become unstable, resulting in a cascade of relaxations called *an avalanche*. It was observed that these models are self-driven into a critical state that is characterized by a set of exponents [1,2]. This set includes the *distribution exponents* that describe the distribution of quantities such as avalanche size, area, and lifetime, and the *geometric exponents* that relate various properties of the dynamics [21,22]. Additional sandpile models that differ from the BTW model in the dynamic rules were introduced and studied. These include the Manna model [29], in which the dynamics during an avalanche is stochastic, and the Zhang model [15], in which the dynamic variable is continuous. In order to understand the basic mechanism of SOC, numerous attempts were made to assign the various models to universality classes. To this end, Vespignani, Zapperi, and Pietronero introduced the fixed scale transformation, which is a real-space renormalization-group (RG) approach [30,31]. They applied this approach to the BTW and Manna models and concluded that these two models belong to the same universality class. Later, a comparison between the critical behavior of BTW and the Manna models was performed, using extensive numerical simulations and an extended set of exponents [32]. The results provide strong evidence that the two models belong to different universality classes. Recently, Diaz-Guilera and Corral applied the dynamic RG technique to study critical behavior in sandpile models. Their conclusion was that the BTW and the Zhang models belong to the same universality class [33–35]. A similar conclusion was reached by Lübeck [36], based on numerical simulations.

In this paper we apply an extended set of tools for the characterization of critical behavior in sandpile models and for their classification into universality classes. These tools include measures that characterize avalanches as a whole such as the distribution exponents, the geometric exponents, and the avalanche structure. We also introduce a measure, based on scaling functions, describing the time evolution of the area, size, and energy during an avalanche. Combining all these tools, we find strong indications that the BTW, Manna, and Zhang models belong to three different universality classes.

The paper is organized as follows. The models are introduced in Sec. II and the measures for their classification are presented in Sec. III. The simulations and results are given in Sec. IV, followed by a summary and conclusions in Sec. V.

II. THE MODELS

Sandpile models are defined on a d-dimensional lattice of linear size L. Each site $\mathbf{i}$ is assigned a dynamic variable $E(\mathbf{i})$, which represents some physical quantity such as energy, stress, etc. In a critical height model a configuration $\{E(\mathbf{i})\}$ is called *stable* if for all sites $E(\mathbf{i})<E_c$, where E_c is a threshold value. The evolution between stable configurations is by the following rules.

(i) *Adding energy*. Given a stable configuration $\{E(\mathbf{j})\}$ we select a site $\mathbf{i}$ at random and increase $E(\mathbf{i})$ by some amount δE. When an unstable configuration is reached rule (ii) is applied.

(ii) *Relaxation rule*. If $E(\mathbf{i})\geqslant E_c$, relaxation takes place and energy is distributed in the following way:

$$E(\mathbf{i})\rightarrow E(\mathbf{i})-\sum_{\mathbf{e}}\Delta E(\mathbf{e}),\quad E(\mathbf{i}+\mathbf{e})\rightarrow E(\mathbf{i}+\mathbf{e})+\Delta E(\mathbf{e}), \tag{1}$$

where $\mathbf{e}$ are a set of (unit) vectors from the site $\mathbf{i}$ to some neighbors. As a result of the relaxation, the dynamic variable

*Electronic address: milstein@flounder.fiz.huji.ac.il
†Electronic address: biham@flounder.fiz.huji.ac.il
‡Electronic address: sorin@vms.huji.ac.il

in one or more of the neighbors may exceed the threshold. The relaxation rule is then applied until a stable configuration is reached. The sequence of relaxations is an avalanche that propagates through the lattice.

It was shown before that the parameters δE and E_c are irrelevant to the scaling behavior [7,33,34]. This indicates that the critical exponents depend only on the vector ΔE, to be termed *relaxation vector*. For a square lattice with relaxation to nearest neighbors (NN), it is of the form $\Delta E = (E_N, E_E, E_S, E_W)$, where E_N, E_E, E_S, and E_W are the amounts transferred to the northern, eastern, southern, and western NN's, respectively. In the BTW model, $E_c = 4$, $\delta E = 1$, and $\Delta E = (1,1,1,1)$. If an active site with $E(\mathbf{i}) > E_c$ is toppled, it would not become empty after the topple had occurred. In the Zhang model [15], for which $E_c = 1$ and $0 < \delta E < 1$, the relaxation vector is given by (b,b,b,b), where $b = E(\mathbf{i})/4$ and $E(\mathbf{i})$ is the amount of energy in the active site before the topple had occurred. Obviously, the site $\mathbf{i}$ remains empty after toppling.

In a random relaxation model [29] a set of neighbors is randomly chosen for relaxation. Such a model is specified by a set of relaxation vectors, each vector being assigned a probability for it application. For example, a possible realization of a two-state model includes six relaxation vectors (1,1,0,0), (1,0,1,0), (1,0,0,1), (0,1,1,0), (0,1,0,1), and (0,0,1,1), each one applied with a probability of 1/6. A four state model would include relaxation vectors such as (4,0,0,0), (3,1,0,0), (2,2,0,0), (2,1,1,0), (1,1,1,1), (0,2,1,1), etc., applied at different probabilities while maintaining the fourfold symmetry of the relaxation rule. A *time step* (of unit *time*) is defined as the relaxation of all the sites having $E(\mathbf{i}) \geqslant E_c$, after the completion of the previous time step. A model is said to be *Abelian* if the configuration after the avalanche does not depend on the order in which the relaxation of the active sites was performed. The BTW model was shown to be Abelian [7]. The Manna models [18,20] are not Abelian because they contain a random choice of the toppling direction. As a result, they develop different scenes of toppling that depend on the order of relaxation of the active sites in a single time step. The Zhang model is also non-Abelian. This can be seen from the following example, when two active NN sites are toppled within the same time step. The site that was toppled last remains empty while the other one is nonempty. This shows that the final configuration depends on the order.

III. MEASURES FOR CLASSIFICATION

Avalanches have various properties that can be measured in a simulation: size, area, lifetime, linear size, and perimeter. The size (s) of an avalanche is the total number of relaxation events that occurred in the course of a single avalanche. The area (a) is the number of sites in the lattice where relaxation occurred. The lifetime (t) of an avalanche is the number of time steps (defined above) that took place during the avalanche. As for the linear size of an avalanche, one can use the radius of gyration (r) of the cluster of sites where relaxation occurred. A site inside the area a is defined as a perimeter site if it has a nearest neighbor where no relaxation took place. The perimeter (p) is the number of perimeter sites. Thus we have a set of variables $\{s,a,t,r,p\}$ that characterize an avalanche. The avalanche variables have probability functions that are assumed to fall off with a power law defined by $P(x) \sim x^{1-\tau_x}$, where $x \in \{s,a,t,r,p\}$ and the exponents τ_x are called *distribution exponents*. These variables also scale against each other in the form

$$y \sim x^{\gamma_{yx}}, \tag{2}$$

for $x,y \in \{s,a,t,r,p\}$ and the exponents γ_{yx} are called *geometric exponents*. The exact definition of the geometric critical exponents γ_{xy} is in terms of conditional expectation values: $E[y|x] \sim x^{\gamma_{yx}}$ [21]. The exponents are not independent. It is shown in [22] that they satisfy the scaling relations

$$\gamma_{yx} = \gamma_{xy}^{-1} \tag{3}$$

and

$$\gamma_{zx} = \gamma_{zy}\gamma_{yx}. \tag{4}$$

Apart from the critical exponents, we have also examined the structural features of the avalanches. We define on the lattice a function that specifies the number of toppling events, $f(\mathbf{i})$, for each site $\mathbf{i}$ during a single avalanche. In a two-dimensional (2D) model this function takes the form of a hilly terrain, with discrete heights. The nth terrace is then defined as the set of sites for which $f(\mathbf{i}) \geqslant n$. This height profile of an avalanche can be described by drawing the area of the nth terrace, A_n vs n. Furthermore, we can consider A_n as an avalanche variable, just like the size or the area, and its distribution is characterized by the exponent $\tau_a(n)$. This gives us new variables that can be measured and compared between the various models.

The avalanche properties introduced so far, such as the area and size, characterize an avalanche as a whole, and are measured only after the avalanche is completed. Here we introduce measures to characterize the time evolution during an avalanche. Measured vs time, for a single avalanche, these measures exhibit an irregular form. However, if we average them over a large number of avalanches, a typical shape emerges. We now introduce three such measures.

(i) The avalanche area $a_c(t)$, namely the number of sites where at least one relaxation occurred during the first t time steps of the avalanche. As the avalanche is completed, $a_c(t)$ evolves to the area a of the avalanche. We also define $a(t)$ as the time derivative of $a_c(t)$, according to $a(t) = da_c(t)/dt$, where $da_c(t)/dt \equiv a_c(t+1) - a_c(t)$. The variable $a(t)$ gives the number of sites that at time t became active for the first time (and are to be toppled in the next time step). As the avalanche evolves to an end we find that the avalanche area satisfies $a = \Sigma_{t=0}^{t_{\max}} a(t)$, where $t_{\max}$ is the avalanche time, and the $t=0$ step consists of the deposition event that initiated the avalanche.

(ii) The number of active sites $s(t)$ (namely sites that are to topple in the next time step) as a function of time. As the avalanche evolves to an end we find that $s = \Sigma_{t=0}^{t_{\max}} s(t)$ is the avalanche size.

(iii) Considering a sandpile in a gravitational field, we define the potential energy $u(t) = \Sigma_{\mathbf{i}} u_{\mathbf{i}}(t)$, where $u_{\mathbf{i}}(t)$ is the energy at site $\mathbf{i}$ given by

$$u_{\mathbf{i}}(t)=\int_0^{E(\mathbf{i})} mgh(t)dh. \tag{5}$$

The values of m and g are irrelevant and we take $mg=1$. The potential energy defined here turns out to be proportional to $E(\mathbf{i})^2$, contrary to the ordinary definition of energy in sandpiles, which is linear in $E(\mathbf{i})$. For the case of a discrete dynamic variable, a site $\mathbf{i}$ having energy $E(\mathbf{i})$ will have a potential energy $u_{\mathbf{i}}(t)=E(\mathbf{i})[E(\mathbf{i})+1]/2$.

Averaging the functions $a(t)$, $s(t)$, and $u(t)$ over a large number of avalanches we obtain the functions $A(t)$, $S(t)$, and $U(t)$, respectively. According to the dynamic scaling assumption, each one of these functions can be written in the general scaling form :

$$X(t)=K_X\langle t\rangle_X^{-\alpha_X} f_X\left(\frac{t}{\langle t\rangle_X}\right), \tag{6}$$

where

$$\langle t\rangle_X=\frac{\sum_t tX(t)}{\sum_t X(t)} \tag{7}$$

and $X\in\{U,S,A\}$. The scaling function $f_X(\mu)$, where $\mu=t/\langle t\rangle_X$, satisfies the sum rules

$$\int_0^\infty f_X(\mu)d\mu=\int_0^\infty \mu f_X(\mu)d\mu=1. \tag{8}$$

The shape of the scaling function and the values of the exponents α_X can be used to distinguish between universality classes. Moreover, the relation between these scaling functions can be used as a further tool. For example, if $f_X(\mu)$ and $f_Y(\mu)$ coincide for one model and are different in another model, it indicates that these two models do not belong to the same universality class. The dependence of $\langle t\rangle_X$ on the system size L is given by

$$\langle t\rangle_X\sim L^{\beta_X}. \tag{9}$$

IV. SIMULATIONS AND RESULTS

Having defined the three models and the measures used for their characterization, we now describe the computer simulations. We have used open boundary conditions and system sizes up to 512^2, with 10^6 to 10^8 grains dropped, in two dimensions (2D). For each run we ascertained, before collecting data, that the dynamics has reached the critical state by applying Dhar's burning algorithm [7], or by starting with a configuration belonging to the critical state. For each model we have calculated all the measures of classification mentioned in Sec. III.

The exponent τ_s that describes the avalanche size distribution was measured for the BTW, Manna four-state, and Zhang models (Fig. 1) finding good agreement with previous results [32,36]. The exponent τ_s for the three models, as a function of the inverse system size, is given in Fig. 2. These results do not provide a reliable extrapolation of τ_s to the infinite system limit. However, they strongly indicate that the curves converge to different values of τ_s as $L\to\infty$. As τ_s exhibits relatively strong dependence on the system size [32], it cannot be used as the primary tool for classification of models, but only to provide additional evidence.

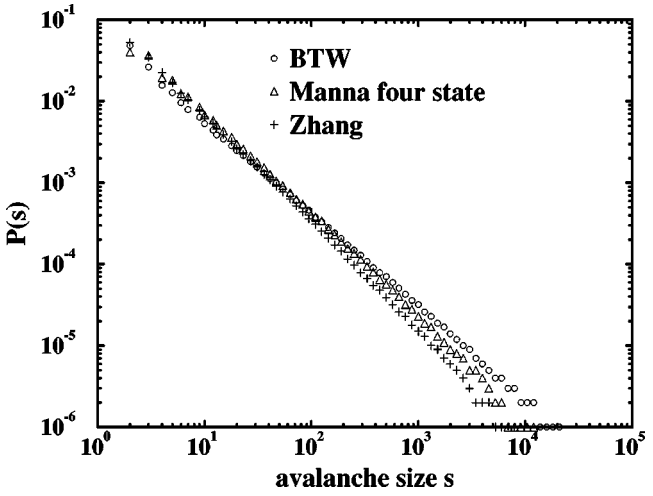

FIG. 1. Avalanche size distributions in the BTW, Manna four-state, and Zhang models. The exponents are $\tau_s=2.090\pm0.005$ for BTW, $\tau_s=2.23\pm0.01$ for Manna, and $\tau_s=2.25\pm0.01$ for the Zhang model. System size is 128^2.

The geometric exponents γ_{xy} are only weakly dependent on the system size, and turn out to be very useful for classification of sandpile models [32]. In our simulations we examined the exponents γ_{sa}, γ_{st}, and γ_{at}. This was done by drawing on a log-log scale quantities such as the average avalanche size $E[s|a]$ for a given area a, where γ_{sa} is given by the slope of the straight line section (Fig. 3). The values of the geometric exponents for the BTW and the Manna four-state models are in agreement with previous simulations [32]. Our simulations of the Zhang model, for system size up

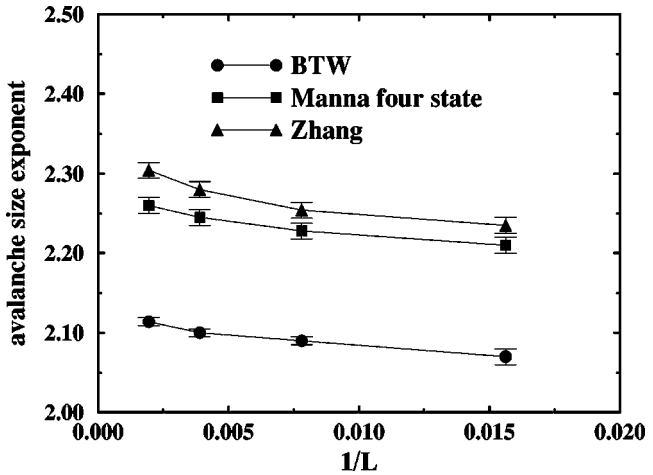

FIG. 2. The exponent τ_s of the avalanche size distribution as a function of the inverse system size $(1/L)$ in the BTW, Manna four-state, and Zhang models. The lines are guides to the eye. Although it is hard to reliably extrapolate from these results to $1/L\to0$, this graph strongly indicates that the curves converge to three different values.

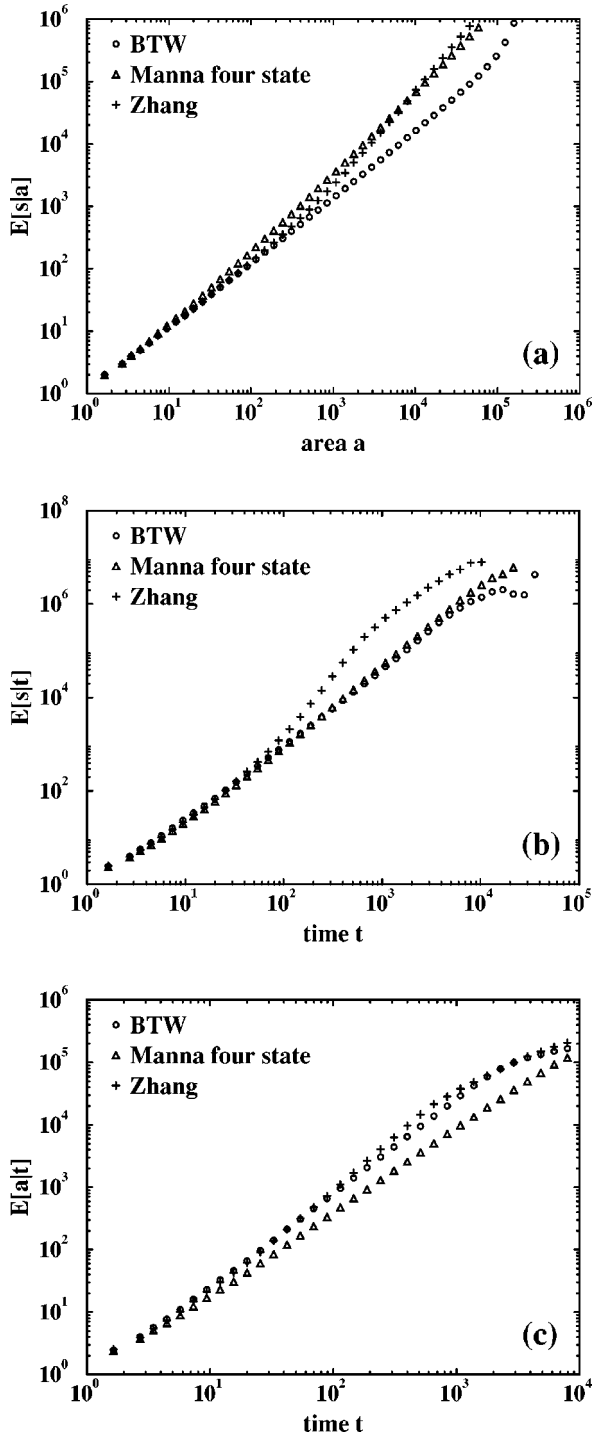

FIG. 3. Geometric critical exponents for the BTW, Manna four-state, and Zhang models. (a) $E[s|a]$ (average avalanche size for given avalanche area) vs a is presented, yielding γ_{sa}. (b) $E[s|t]$ is given vs t (avalanche time), yielding γ_{st}. (c) $E[a|t]$ is given vs t, yielding γ_{at}. System size is 512^2 with 10^7 grains dropped. Data were binned with uniform bin sizes on the logarithmic scale.

to 1024^2, showed that these variables, γ_{sa}, γ_{st}, and γ_{at}, *are not scale invariant* (Fig. 3). Although for small avalanches the scaling behavior for the Zhang model resembles the distribution of the same variables in the BTW model, for large avalanches we find a *bend* and a sudden change in slope. This bend is insensitive to the system size for all the system sizes that were checked (Fig. 4). For large avalanches, the

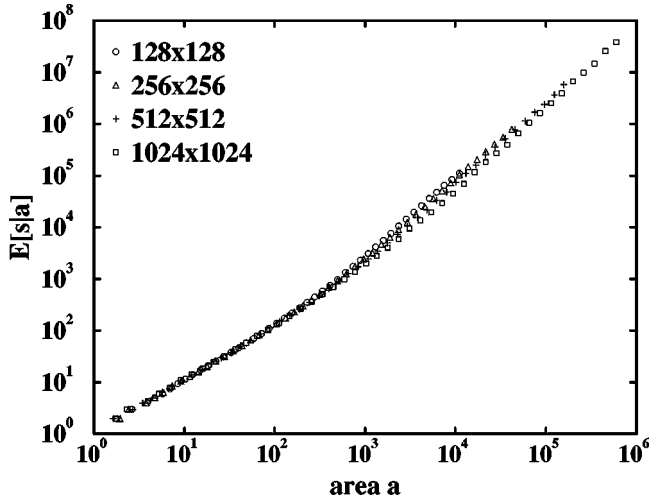

FIG. 4. The conditional expectation value $E[s|a]$ vs a, which yields γ_{sa} for the Zhang model for four system sizes between 128^2 and 1024^2. A bend is observed below which γ_{sa} is similar to the corresponding exponent for the BTW model. Above this bend $\gamma_{sa}=1.60\pm0.05$. This value is clearly different from the $\gamma_{sa}=1.05\pm0.01$ of the BTW model and the $\gamma_{sa}=1.240\pm0.005$ for the Manna four-state model.

geometric exponents are clearly different from the values recorded for the BTW model and for the Manna four-state model. This puts in question the previous assignment of the Zhang model to the universality class of the BTW model [33–36].

To further characterize the avalanche structure, we examined the function $f(\mathbf{i})$, which provides the number of toppling events at site $\mathbf{i}$ during the avalanche (Fig. 5). For the BTW model, we observe a shell structure in which all sites that relaxed at least $n+1$ times form a connected cluster with no holes, which is contained in the cluster of sites that relaxed at least n times [7,37]. The Manna four-state model exhibits a random avalanche structure with many peaks and holes [32]. In between we find the Zhang model, which shows an avalanche structure that is mostly shelled, but is different from the BTW picture by having several peaks and holes, but not as many as in the Manna four-state model.

To obtain a more quantitative characterization of the terrace structure we chose typical large avalanches for each of the three models and plotted the terrace number n as a function of its area (Fig. 6). For the Manna model this function exhibits higher and sharper peak compared to the two other models. We have also measured, for the three models, the distribution exponents $\tau_a(n)$ for terraces no. 2, 3, 4, and 5 (Table I). The results show quantitative differences in the avalanche structures, between the three models. In all cases $\tau_a(n)$ decreases as n is increased. The differences are significant with the lowest $\tau_a(n)$ for Zhang, intermediate for BTW, and highest for Manna models.

To obtain a more complete characterization of critical behavior in sandpile models we also examine the time evolution of the energy, avalanche size, and area during the avalanche, averaged over a large number of avalanches. Combining results for system sizes $L=128$, 256, and 512 we draw the scaling functions $f_U(\mu)$, $f_S(\mu)$, and $f_A(\mu)$ that describe the averaged time evolution of the energy, number of active sites, and area growth rate during the avalanche.

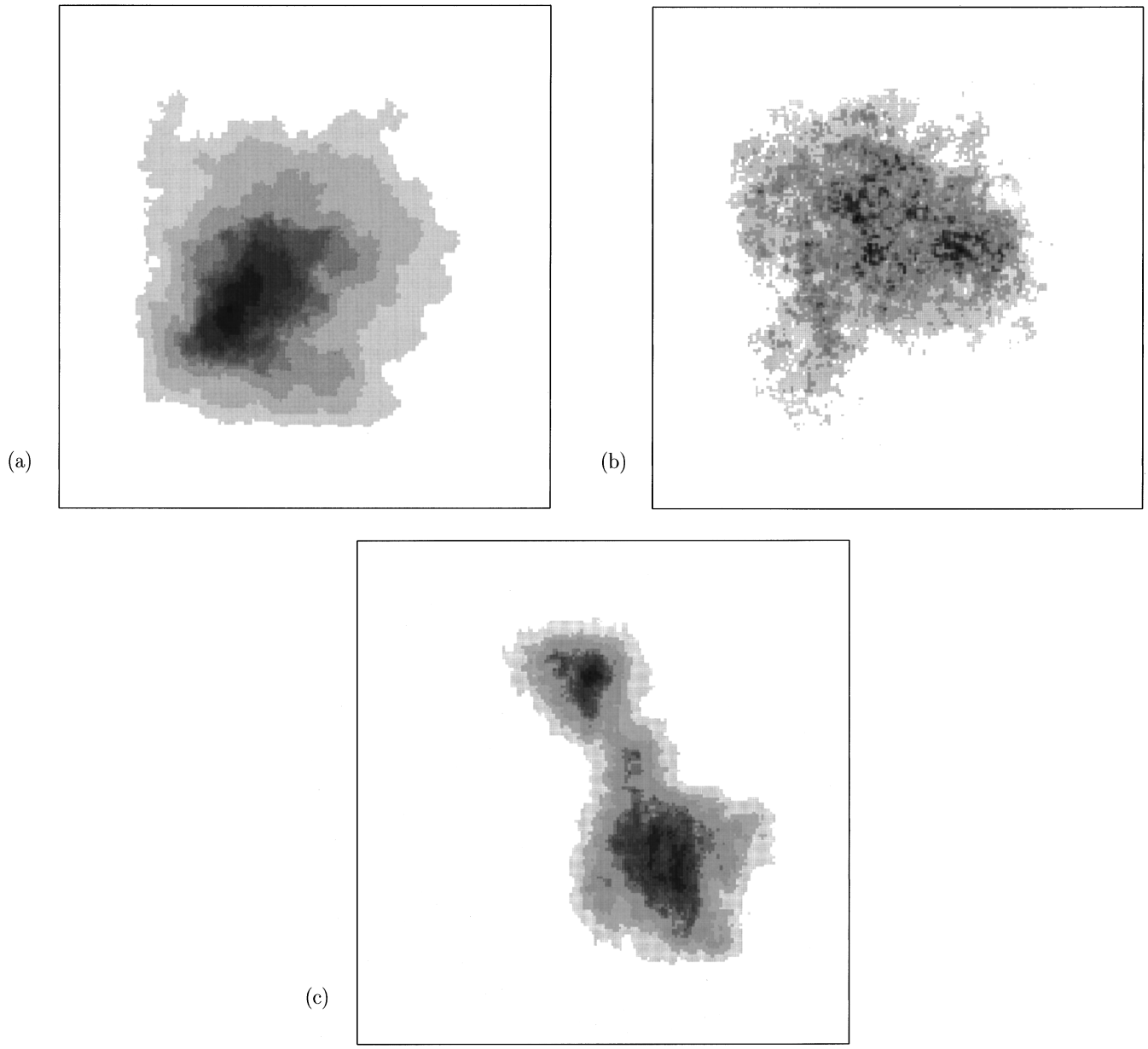

FIG. 5. Typical large avalanche structure for the BTW model (a), Manna four-state model (b), and the Zhang model (c). Gray scales indicate the number of toppling events $f(\mathbf{i})$ that occurred at each site during the avalanche. White represents zero relaxations, and black represents the maximal number of relaxations [13 in (a), 16 in (b), and 17 in (c)]. System size is 128^2. Note the shell structure in the BTW avalanche [4] vs the irregular structure of the avalanche in the Manna four-state model, and the intermediate structure of the Zhang avalanche. These qualitative geometrical differences translate into quantitative differences in exponent values.

The scaling functions for the BTW, Manna, and Zhang models are shown in Figs. 7, 8 and 9, respectively. For the BTW and Manna models we find excellent data collapse indicating scaling behavior. No such scaling is found for the Zhang model, indicating that it lacks some of the features of a critical system, which are found in the BTW and Manna models. For the BTW model (Fig. 7) we observe that all three scaling functions $f_U(\mu)$, $f_S(\mu)$, and $f_A(\mu)$ are identical, so the system is basically described by a single scaling function. For the Manna model, we find that $f_U(\mu)$ and $f_S(\mu)$ coincide, while $f_A(\mu)$ is different. For the Zhang model, we find that there is no data collapse and therefore no scaling function. Interestingly, for each system size the functions $f_U(\mu)$ and $f_S(\mu)$ are identical, while $f_A(\mu)$ is different. The average times are found to depend on the system size according to $\langle t\rangle_X \sim L^{\beta_X}$, where $X \in \{U,S,A\}$. For the BTW model, $\beta_U = 1.51$, $\beta_S = 1.43$, and $\beta_A = 1.31$; for the Manna model, $\beta_U = 1.52$, $\beta_S = 1.53$, and $\beta_A = 1.48$; for the Zhang model one can approximate these exponents by values $\beta_U = 1.5$, $\beta_S = 1.46$, and $\beta_A = 1.36$ but there is a significant deviation from a straight line in the log-log plots of $\langle t\rangle_X$ vs L.

V. SUMMARY AND CONCLUSIONS

We have studied universality in isotropic, Abelian, and non-Abelian sandpile models using a combination of extensive numerical simulations and an extended set of measures

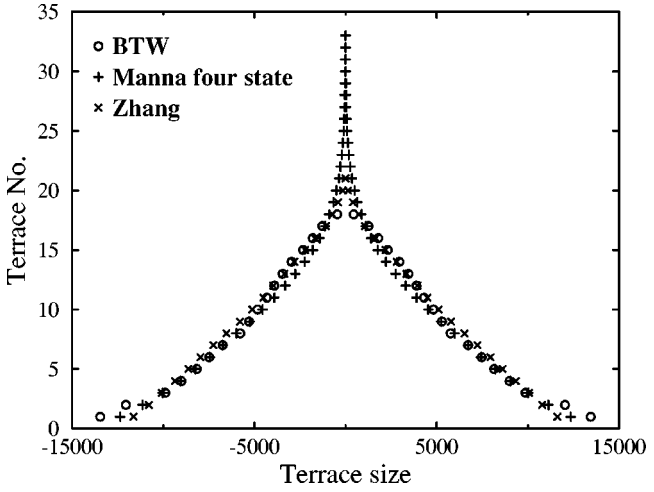

FIG. 6. The activity profile of a typical large avalanche in the BTW, Manna four-state and Zhang model. The terrace number is plotted as a function of its area. The picture is reflected around the y axis. The system size is 128^2. The BTW and Zhang models exhibit moderate slopes, while in the Manna four-state model the slope becomes extremely steep at high terrace numbers.

to characterize these models. In particular, we focused on the BTW model (which is Abelian, deterministic, and isotropic), the Manna model (non-Abelian, stochastic, and isotropic on average), and the Zhang model (non-Abelian, deterministic, and isotropic). For each model we have calculated the critical exponents that characterize an avalanche as a whole. These include the distribution exponents τ_x, which characterize the distribution of quantities such as avalanche size, area, and lifetime, and the geometric exponents γ_{xy}, which relate the scaling properties of different quantities. The geometric exponents γ_{xy} are particularly useful for classification due to their weak dependence on the system size. Comparing these exponents we find clear indications that the BTW and Manna models belong to different universality classes, in agreement with previous simulations [32]. As for the Zhang model, the geometric critical exponents are not well defined. For all system sizes examined, the functions $E[y|x]$ vs x, where $x,y \in \{s,a,t\}$, from which the exponents γ_{xy} are obtained, exhibit domains with different slopes for small and large avalanches. The small avalanche behavior is similar to the BTW results, while the large avalanche behavior is different from both the BTW and Manna models.

TABLE I. The distribution exponent $\tau_a(n)$ for the areas of the terraces no. $n=2,3,4,5$, in a 2D sandpile of size 128^2. For all three models, $\tau_a(n)$ tends to decrease as the terrace order n increases. The differences between the models are significant, with the lowest exponents for Zhang, intermediate for BTW, and highest for the Manna model.

Exponent	model		
	BTW	Manna four-state	Zhang
$\tau_a(2)$	2.05 ± 0.03	2.16 ± 0.03	1.98 ± 0.03
$\tau_a(3)$	2.00 ± 0.04	2.11 ± 0.04	1.85 ± 0.04
$\tau_a(4)$	1.95 ± 0.05	2.09 ± 0.05	1.77 ± 0.05
$\tau_a(5)$	1.91 ± 0.05	2.00 ± 0.05	1.74 ± 0.05

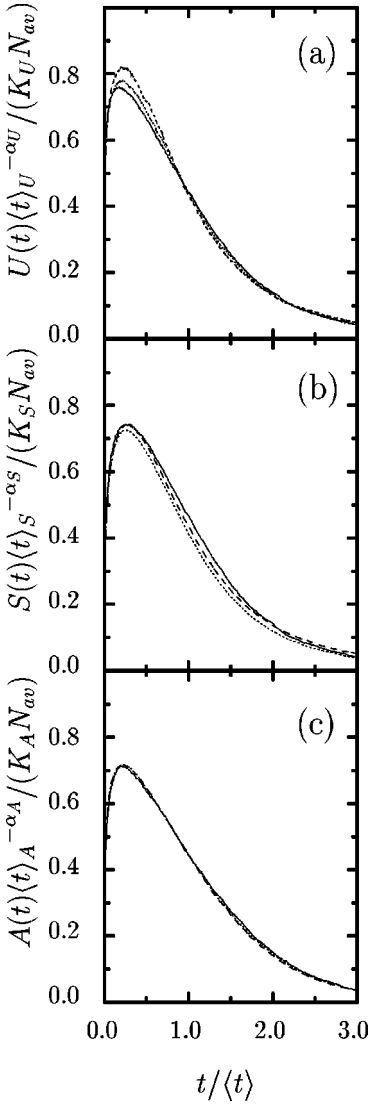

FIG. 7. The scaling functions for the BTW model for $L=128$, 256, and 512: (a) $f_U(\mu)$, which describes the time dependence of the energy during the avalanche; (b) $f_S(\mu)$, which describes the time dependence of the number of active sites; and (c) $f_A(\mu)$ which describes the time dependence of the avalanche area growth rate. We observe that all three scaling functions coincide, indicating a common scaling function for U, S, and A. The exponents are found to be $\alpha_U=0.24$, $\alpha_S=0.39$, and $\alpha_A=0.26$ and the prefactors $K_U=2.34$, $K_S=0.3$, and $K_A=0.55$.

The avalanche structures of the three models are found to be significantly different. The BTW avalanche structure is the most regular, the Manna structure is the most irregular, and the Zhang avalanche structure is intermediate.

We have also examined measures of the dynamics during the avalanche. We found scaling functions for the time evolutions of the energy $f_U(\mu)$, number of active sites $f_S(\mu)$, and the rate of area growth $f_A(\mu)$ in the BTW and Manna models. For the BTW model, all three scaling functions coincide, while for the Manna model only the first two coincide. This is a qualitative difference that further strengthens our conclusion that the two models belong to different universality classes. For the Zhang model these functions do not exhibit scaling behavior. This is a further indication that the Zhang model lacks some essential features of critical behavior, which appear in the BTW and Manna models, and thus

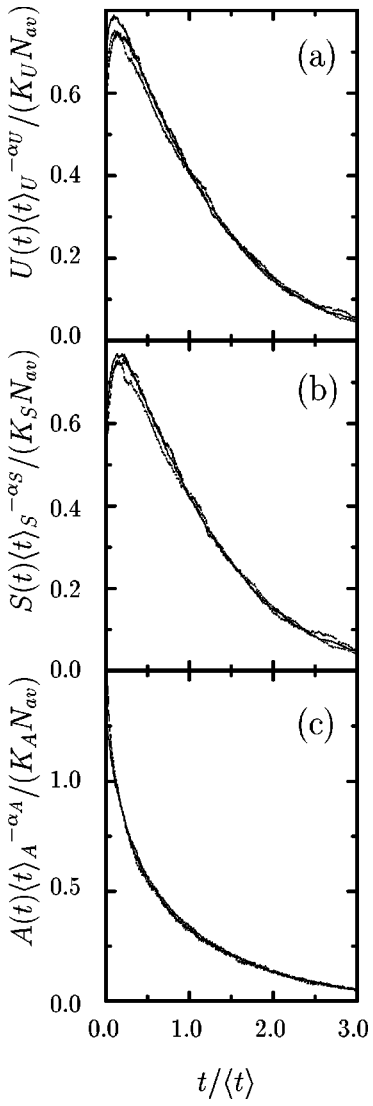

FIG. 8. The scaling functions for the Manna four-state model for $L=128$, 256, and 512: (a) $f_U(\mu)$, (b) $f_S(\mu)$, and (c) $f_A(\mu)$. We observe that the scaling functions $f_U(\mu)$ and $f_S(\mu)$ coincide while $f_A(\mu)$ has a completely different form. The exponents are found to be $\alpha_U=0.24$, $\alpha_S=0.3$, and $\alpha_A=-0.11$ and the prefactors $K_U=1.76$, $K_S=0.221$, and $K_A=0.93$.

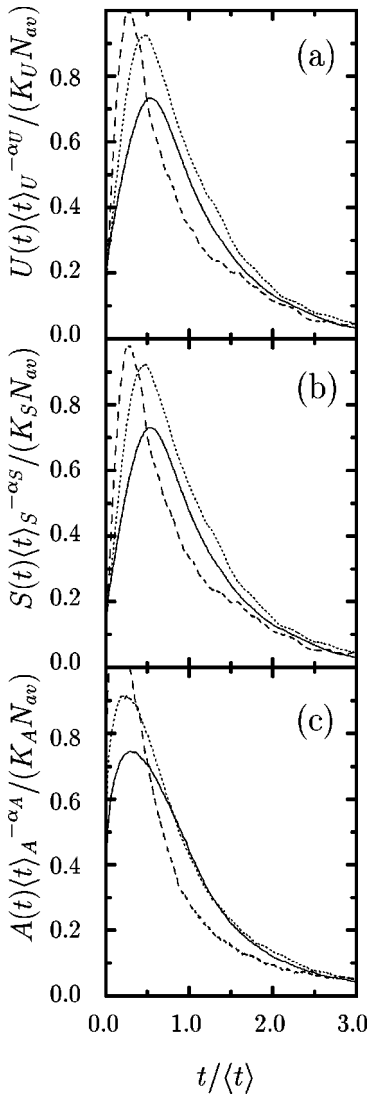

FIG. 9. The functions (a) $f_U(\mu)$, (b) $f_S(\mu)$, and (c) $f_A(\mu)$ for the Zhang model for $L=128$, 256, and 512. We observe that functions obtained from different system sizes do not coincide, indicating that these are not scaling functions. This indicates that the Zhang model lacks some of the characteristic features of a critical state found in the BTW and Manna models. Interestingly, for each system size $f_U(\mu)$ and $f_S(\mu)$ still coincide, while $f_A(\mu)$ is different. The exponents are found to be $\alpha_U=0.3$, $\alpha_S=0.32$, and $\alpha_A=-0.2$ and the prefactors $K_U=0.55$, $K_S=0.76$, and $K_A=3.55$.

belongs to a different universality class. In fact, the only unambiguous scaling features of the Zhang model are given by the distribution exponents τ_x. We thus conclude that the BTW, Manna, and Zhang models belong to three universality classes.

Our results disagree with the conclusions of a number of recent studies. Lübeck studied the scaling behavior in the BTW and Zhang models using extensive numerical simulations [36]. Relying only on the distribution exponents, he concluded that the BTW and Zhang models belong to the same universality class. As we demonstrated above, the distribution exponents provide very limited characterization of the scaling behavior. Therefore, these exponents alone are not enough to support a conclusion that two models belong to the same universality class. Moreover, the distribution exponents are strongly dependent on the system size. One should be careful in interpreting the results of the finite size analysis done in [36], based on an assumed size dependence that is not substantiated theoretically. Recently Corral and Diaz-Guilera derived nonlinear partial differential equations based on the microscopic evolution rules of the BTW and Zhang models [35]. Using a dynamic RG approach they analyzed these equations and concluded that the two models belong to the same universality class. Vespignani, Zapperi, and Pietronero used a real space RG approach and concluded that the BTW and Manna models belong to the same universality class [30,31]. The failure of these approaches to distinguish between the universality classes indicates that some key ingredients of the dynamics are not taken into account.

The results presented here provide a further indication for the rich and diverse behavior of sandpile models. On the one hand, the fact that so many different models exhibit scaling behavior shows that the self-organized critical state is ge-

neric for a broad class of slowly driven systems. On the other hand, the critical exponents and scaling functions are found to be dependent on details of the model dynamics. We speculate that these details may be related to symmetries such as the Abelian symmetry, as well as properties such as the deterministic vs stochastic nature of the avalanche dynamics. Revealing the relation between the scaling properties and the underlying symmetries would open the way to a systematic classification of these systems, and to the complete RG-type theory of SOC. Furthermore, applying the measures introduced here in the analysis of experimental results may sharpen the experimental evidance for SOC in empirical systems.

ACKNOWLEDGMENTS

We thank M. Paczuski for helpful discussions and correspondence.

[1] P. Bak, C. Tang, and K. Wiesenfeld, Phys. Rev. Lett. **59**, 381 (1987).
[2] P. Bak, C. Tang, and K. Wiesenfeld, Phys. Rev. A **38**, 364 (1988).
[3] C. Tang and P. Bak, Phys. Rev. Lett. **60**, 2347 (1988).
[4] D. Dhar and R. Ramaswamy, Phys. Rev. Lett. **63**, 1659 (1989).
[5] T. Hwa and M. Kardar, Phys. Rev. Lett. **62**, 1813 (1989).
[6] T. Hwa and M. Kardar, Physica D **38**, 198 (1989).
[7] D. Dhar, Phys. Rev. Lett. **64**, 1613 (1990).
[8] J. M. Carlson, J. T. Chayes, E. R. Grannan, and G. H. Swindle, Phys. Rev. A **42**, 2467 (1990).
[9] G. Grinstein, D.-H. Lee, and S. Sachdev, Phys. Rev. Lett. **64**, 1927 (1990).
[10] J. M. Carlson, J. T. Chayes, E. R. Grannan, and G. H. Swindle, Phys. Rev. Lett. **65**, 2547 (1990).
[11] G. Grinstein and D.-H. Lee, Phys. Rev. Lett. **66**, 177 (1991).
[12] L. Pietronero, P. Tartaglia, and Y.-C. Zhang, Physica A **173**, 22 (1991).
[13] S.-C. Lee, N. Y. Liang, and W.-J. Tzeng, Phys. Rev. Lett. **67**, 1479 (1991).
[14] M. Paczuski and S. Boettcher, Phys. Rev. Lett. **77**, 111 (1996).
[15] Y. C. Zhang, Phys. Rev. Lett. **63**, 470 (1989).
[16] L. P. Kadanoff, S. R. Nagel, L. Wu, and S.-M. Zhou, Phys. Rev. A **39**, 6524 (1989).
[17] P. Grassberger and S. S. Manna, J. Phys. (Paris) **51**, 1077 (1990).
[18] S. S. Manna, J. Stat. Phys. **59**, 509 (1990).
[19] S. S. Manna, L. B. Kiss, and J. Kertesz, J. Stat. Phys. **61**, 923 (1990).
[20] S. S. Manna, Physica A **179**, 249 (1991).
[21] K. Christensen, H. C. Fogedby, and H. J. Jensen, J. Stat. Phys. **63**, 653 (1991).
[22] K. Christensen and Z. Olami, Phys. Rev. E **48**, 3361 (1993).
[23] J. Rajchenbach, Phys. Rev. Lett. **65**, 2221 (1990).
[24] G. A. Held, D. H. Solina II, D. T. Keane, W. J. Haag, P. M. Horn, and G. Grinstein, Phys. Rev. Lett. **65**, 1120 (1990).
[25] C.-H. Liu, H. M. Jaeger, and S. R. Nagel, Phys. Rev. A **43**, 7091 (1991).
[26] S. Nagel, Rev. Mod. Phys. **64**, 321 (1992).
[27] S. Ciliberto and C. Laroche, J. Phys. I **4**, 223 (1994).
[28] V. Frette, K. Christensen, A. M.-Sørenssen, J. Feder, T. Jøssang, and P. Meakin, Nature (London) **379**, 4 (1996).
[29] S. S. Manna, J. Phys. A **24**, L363 (1991).
[30] A. Vespignani, S. Zapperi, and L. Pietronero, Phys. Rev. Lett. **72**, 1690 (1994).
[31] A. Vespignani, S. Zapperi, and L. Pietronero, Phys. Rev. E **51**, 1711 (1995).
[32] A. Ben-Hur and O. Biham, Phys. Rev. E **53**, R1317 (1996).
[33] A. Diaz-Guilera, Phys. Rev. A **45**, 8551 (1992).
[34] A. Diaz-Guilera, Europhys. Lett. **26**, 177 (1994).
[35] A. Corral and A. Diaz-Guilera, Phys. Rev. E **55**, 2434 (1997).
[36] S. Lübeck, Phys. Rev. E **56**, 1590 (1997).
[37] E. V. Ivashkevich, D. V. Ktitarev, and V. B. Priezzhev, Physica A **209**, 347 (1994).